Tabriz Journal of Electrical Engineering (TJEE), vol. 56, no. 1, 2026 Serial no. 115
DOI: 10.22034/tjee.2026.69036.5080

A novel power divider network with momentum matching for feeding arrays of arbitrary spoof surface plasmon polaritons antennas

M. Siasifar[1], A. Keshtkar[1*], S. Amiri[2]

[1] Faculty of Technical and Engineering, Imam Khomeini International University, Qazvin, Iran, 34148-96818.
[2] Electrical Engineering Department of Iranian Research Organization for Science and Technology (IROST), Tehran, Iran, 3313193685.
E-mail addresses: msiasifar@gmail.com, akeshtkar@gmail.com*, amiri@irost.ir

Received: 23/09/2025, Revised: 06/12/2025, Accepted: 13/01/2026.

Abstract
A novel power divider network for feeding arrays of arbitrary groundless spoof surface plasmon polaritons (SSPP) antennas with coplanar waveguide (CPW) input is proposed. The design approach is generalized for any SSPP antenna with CPW input by presenting a flowchart. The proposed feeding network is simulated and optimized via CST Studio software. We validate our designed network's effectiveness using a fabricated prototype eight-branch SSPP array antenna that shows a measured impedance bandwidth of 0.98 GHz (11.536-12.516 GHz) and a maximum gain increase of 7.48 dB compared with a single-branch SSPP antenna, with only a 1.55 dB deviation from the lossless theoretical increase value of 9.03 dB. The proposed power divider network can feed SSPP antennas with no attached ground, enabling performance optimization of the antenna by placing a detached ground. Planar antennas, especially SSPP-based antennas, are increasingly favored in satellite and aerospace applications because of their lightweight, low-profile, and conformal nature, enabling seamless integration into rockets and satellites. Their high efficiency, wideband operation, and low loss (enhanced by SSPP structures) support high-speed communications, whereas beam steering and electromagnetic interference resilience make them ideal for dynamic aerospace environments. However, since many SSPP antennas use CPW inputs and single-branch SSPP antennas often lack sufficient gain, the efficient power divider network proposed in this paper holds particular importance for combining multiple radiating elements, boosting gain and directivity without compromising compactness. These advantages align perfectly with the demands of next generation satellite and terrestrial communication systems, and unmanned aerial vehicles (UAVs).

Keywords
Microstrip to CPW transition, planar antennas, plasmonics, power divider networks, spoof surface plasmon polaritons (SSPP) antennas, array antennas.

1. Introduction

Telecommunications technology has recently witnessed an increase in the demand for flat panel systems including planar antennas, both in modern terrestrial telecommunications networks such as fifth and sixth generation (5G and 6G) telecommunications and in constellations of low-Earth orbit (LEO) non-geostationary (NGSO) telecommunications satellites. The main objective of these new communication systems is to connect anyone and anything anywhere that, in the majority of cases, is only mechanically possible if a planar microwave antenna structure is used. NGSO satellites that are equipped with small, compact, and deployable planar antennas can be launched with more economic scenarios when several satellites are stored in a large rocket or when a single satellite is launched in rockets with smaller diameters. Additionally, the need for the miniaturization of electronic devices has raised the quest for compact, thin, planar, and low-profile microwave circuits. Structures enabling surface wave propagation represent one of the most efficient solutions for manufacturing low-profile microwave devices. The proper design of such structures can confine the waves in the vicinity of the circuit surface and create a propagating wave with low attenuation across the surface and exponential degradation in the perpendicular direction. Such propagation creates an ideal waveguide that not only has low loss and high-power efficiency, but also lacks unwanted coupling and interference and has good electromagnetic compatibility (EMC). As metals exhibit negative permittivity at THz and optical frequencies, dielectrics coated with metals have opposite permittivities at the metal-dielectric interface and can create strictly confined surface waves in the interface area, which are called surface plasmon polaritons (SPPs) [1]. At microwave frequencies, metals behave as perfect electric conductors (PECs) without negative permittivity, preventing the generation of SPPs. However, research have demonstrated that engineered structures with holes or corrugations can artificially mimic plasmonic effects. These artificial SPPs are called "spoof" SPPs (SSPPs) and can exhibit controllable dispersion characteristics and operate effectively not only at optical frequencies but also in the microwave regime, enabling surface wave propagation in frequency ranges where natural SPPs cannot exist [2]. Further studies have shown that SSPPs

are good candidates for fabricating many planar and low-profile microwave devices, including ultrathin low-loss planar single-conductor waveguides that can efficiently guide surface waves [3]. An efficient single-conductor SSPP waveguide is also widely used in different planar antennas, including SSPP leaky wave antennas. Planar antennas, especially SSPP-based antennas, are increasingly favoured in satellite and aerospace applications because of their light weight, low-profile, and conformal nature, enabling seamless integration into rockets and satellites. Their high efficiency, wideband operation, and low loss (enhanced by SSPP structures) support high-speed communications, whereas beam steering and electromagnetic interference (EMI) resilience make them ideal for dynamic aerospace environments. The input/output circuits of conventional microwave devices use two-conductor waveguides, such as microstrip or coplanar waveguides (CPWs), with quasi-TEM propagation modes different from those of single-conductor SSPP waveguides. Therefore, to connect conventional devices with two conductor waveguide interfaces to SSPP waveguides, we need to consider mode and momentum conversion as well as impedance matching [4]. The method introduced in [4] for interfacing between conventional circuits and SSPP waveguides via a CPW is both broadband and efficient and is therefore used in many SSPP circuits, including single-branch SSPP planar antennas. Unlike microstrip lines, which require dual-sided boards, CPW uses only one layer, eliminating the need for an attached bottom ground to the SSPP antenna, which allows the placement of a PEC or artificial magnetic conductor (AMC) ground plane at an optimized distance from the antenna - a critical advantage since close proximity between radiators and attached grounds degrades high-frequency performance [5-7]. This benefit further validates the structural choice presented in this paper for SSPP antennas. However, since single-branch SSPP antennas often lack sufficient gain, in high-gain antenna systems requiring array configurations, the implementation of a matched power divider for feeding array branches becomes inevitable. Therefore, an efficient power divider network, designed specifically for a single-conductor SSPP input waveguide of the array branches with optimal power distribution and minimal loss and proper phase coherence across all radiating elements, holds particular importance for combining multiple radiating elements, boosting gain and directivity without compromising compactness. In the case of SSPP antenna arrays, the output ports of the power divider should be matched to the mode and momentum conversion mechanism of each SSPP antenna branch, which is more complicated than conventional dividers used in other array antennas. In this paper, we propose an efficient generalized method for designing a novel network of power dividers that can be efficiently used in any arbitrary multibranch SSPP antenna array that uses the wide band and efficient CPW input introduced in [4].

The rest of this paper is organized as follows: Section 2 describes the general design process and analysis of the eight-branch planar power divider and mode and momentum matching network for multibranch SSPP array antennas and its components. Section 3 discusses the simulation and experimental evaluation of the proposed divider network. Section 4 presents the conclusion of this work.

2. General Design Process and Analysis

2.1. General Structure and Interfacing Sections

The initial step in interfacing between double conductor conventional waveguides and groundless SSPP single-conductor waveguides is eliminating the input ground conductor. The method used in [4] and similar papers supposes that the second ground conductor of SSPP is located at infinity and uses a tapered structure to gradually direct the CPW ground to infinity. Figure 1 shows the general structure of a typical converting section of a double-conductor CPW input to a single-conductor SSPP waveguide. The input section of Fig. 1 is a conventional two conductor CPW waveguide over a dielectric layer with a dielectric relative permittivity ε_r and a central conductor width of the W_{CPW} and two ground conductors located in the same layer with a gap space of g. The single-conductor SSPP waveguide is connected to the other side of the CPW waveguide, which has two tapered grounds. Most SSPP structures use a gradual transition from a CPW to a SSPP single-conductor waveguide [8], but some SSPP types, such as the periodic hole etched on the CPW middle conductor proposed in [9], use a sudden transition between the CPW and SSPP. Although the structure in Fig. 1 is very effective and straightforward for single-branch circuits, when multiple branches are used side by side, collision between lateral tapered grounds and other circuit elements require special spatial arrangements. In other words, as the lateral tapered ground shown in Fig. 1 collide with the adjacent antenna branches, therefore a novel structure that avoids such collisions and provides the required ground connection for each branch should be designed to overcome this problem. In this paper, we propose an efficient power divider network for an arbitrary multibranch SSPP antenna array with CPW input. A promising first approach for designing an efficient divider network is implementing an SSPP divider that maintains consistent propagation characteristics with the antenna SSPP waveguide, thus eliminating multiple mode conversion requirements. The spacing requirements between SSPP divider branches are inherently dependent on the overall geometric configuration of the SSPP structure, which creates fundamental limitations for miniaturization in multibranch SSPP antenna designs. While optimal low branch separation distances are crucial for achieving the high array factor characteristics, the physical constraints

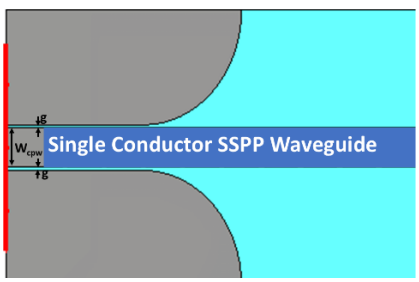

Fig. 1. The general structure of a typical double-conductor CPW to single-conductor SSPP converting section.

imposed by the SSPP geometry often prevent reduction to arbitrarily small dimensions. The maximum array factor is achieved when branch distances equal to divider spacing are more diminutive or near one wavelength [10]. Achieving such a small separation distance in SSPP dividers typically results in significant power division losses. Although we study several proposed SSPP dividers [11-13], our simulations show that the geometry of these SSPP dividers uses a gradual transition from one branch into two or more branches and imposes high division losses when we use them in closely spaced antenna branches with nongradual transitions. Consequently, conventional dividers are a better choice than SSPP-based dividers for feeding multibranch SSPP array antennas. While the CPW power divider represents a potential alternative, its design parameters result in impractical dimensions for fabrication at most microwave frequency ranges. Another conventional power divider that is efficiently used in many microwave applications is the microstrip power divider. In microstrip designs, the ground plane resides on a separate layer beneath the transmission line, whereas in the input CPW structures of SSPP antennas, the ground conductors are positioned on the same plane as the signal line. Consequently, the resulting electric field distributions in these two transmission line structures are nearly orthogonal. To connect the output of the microstrip power divider to the input of the CPW port of the SSPP antenna, we need a special circuit to match the ground and field geometry of the two waveguides and their impedances. Among the several designs employing diverse principles that have been introduced to facilitate microstrip-to-CPW transitions [14-17], the circuit proposed in Fig. 6 of [17] stands out as a good candidate for interfacing SSPP antennas with the CPW input. For our design, we choose the middle band frequency and free space wavelength of f_0=11.95 GHz and λ_0 =25.1 mm, respectively. We employ the frequency-domain solver in CST Studio to simulate and optimize the S-parameters across all sections of our feeding network. For all the circuits in this paper, we use a Rogers RO4003C® substrate with a dielectric relative permittivity (ε_r), loss tangent and thickness (t_d) of 3.55, 0.0027 and 0.813 mm, respectively, to construct an SSPP waveguide with the unit cell configuration shown in Fig. 2(a,b) and the dispersion curve shown in Fig. 2(c). The copper thickness (t_m) is 35 µm in all circuits.

2.2. *Microstrip to CPW transition Circuit*

The microstrip to CPW transition circuit is presented in a dual-layer configuration, with Fig. 3(a) illustrating the upper surface and Fig. 3(b) depicting the lower surface layout. Table I shows the values of the optimized parameters of various parts of the elements in Fig. 3.

2.3. *Power Divider Section*

Our simulations also show that among several proposed microstrip power dividers, the compact multistep quarter wavelength microstrip power divider designed and optimized according to the methods described in [19] fits our requirements. As the input bottom layer microstrip ground is limited to a small portion of the input section

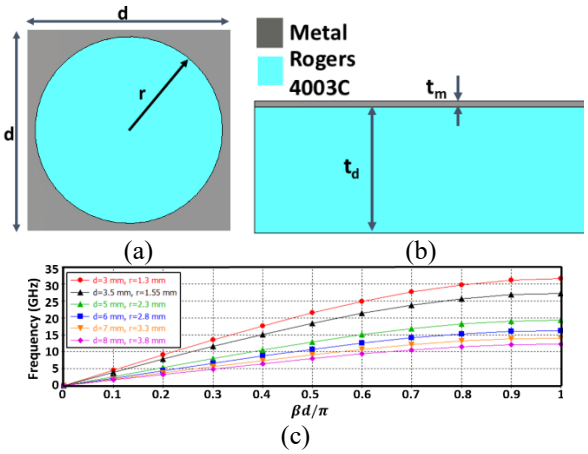

Fig. 2. Unit cell (a) top view (b) side view, t_d=0.813 mm, t_m=35 µm [18] and, (c) dispersion curve of the unit cell for the Rogers RO4003C® substrate (ε_r=3.55, loss tangent of 0.0027), with some different values of d and r in mm.

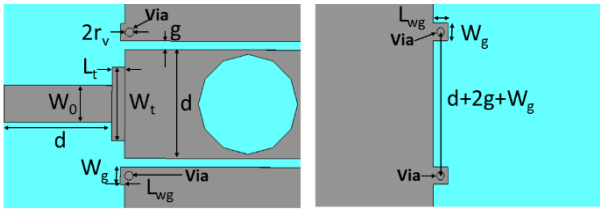

Fig. 3. (a) Top layer and (b) bottom layer layout and parameters of the microstrip to CPW transition circuit.

Table I. Values of the parameters of Fig. 3, all in millimeters

W_0	W_g	W_t	r_v	L_t	L_{wg}	d
1.7	0.8	3.4	0.2	0.6	0.2	5

with dimensions near the free space wavelength (λ_0), the process of designing microstrip power dividers for SSPP waveguides with CPW input is not straightforward because of the possibility of creating unwanted resonance, and special precautions are necessary. While theoretical calculations suggest that the number of matching steps in the power divider could be optimized on the basis of solely the divider bandwidth requirements, our simulation reveals unexpected resonance issues that necessitate both increasing the number of matching steps beyond theoretical predictions and carefully positioning the steps in horizontal or vertical signal paths. As shown in Fig. 3(b), the bottom layer of the transition section has two parts. The first part that is under the microstrip is a two-layer circuit with ground on the bottom, and the second part is a one-layer circuit with a CPW ground on the top layer that is connected by a metallic via to the microstrip ground in the bottom layer. When the number of branches of the antenna array increases, multiple layers of power dividers are needed for feeding. Notably, since the divider network is a non-radiating component, its length must be minimized to avoid compromising the overall antenna efficiency. Consequently, while multiple quarter-wavelength sections can be implemented in either the vertical or horizontal segments of the divider branches (when physically feasible), vertical placement is generally favoured to avoid increasing the antenna's lateral

dimensions. For configurations involving more than two antenna branches, multiple dividers become necessary. In such cases, the microstrip branch lengths incrementally increase with each additional divider stage following the primary divider that connects adjacent antenna branches. This configuration results in an extended microstrip waveguide input section with an accompanying ground plane, which can form resonant structures that trap propagating waves and significantly alter the S-parameters when the circuit dimensions approach integer multiples of $\lambda_0/2$. Any change in the circuit dimensions or its equivalent capacitance or inductance may move the resonance frequency outside the operating bandwidth. Therefore, to eliminate unwanted resonance inside the operational bandwidth, we can change the position of quarter wavelength sections in the vertical or horizontal parts of the power divider or increase the number of steps. Since this procedure includes iterative trial and error attempts, we use the flowchart shown in Fig. 4 to systematically develop power dividers for each section. As illustrated in Fig. 4, our design methodology begins with a single-section power divider (N=1) and iteratively adds quarter-wavelength matching stages until optimal S-parameter performance is achieved across the entire operational bandwidth. Then, we calculate the length of each branch of the power divider according to its position in multiple layers of the power division network, attempt to locate the quarter wavelength sections in the vertical branches, simulate the design with actual values and check the S parameters for unwanted resonance in the entire required bandwidth. If the S parameters are satisfactory, we proceed to the next power divider. If the S parameters are not acceptable, we attempt to locate one of the N quarter wavelength sections in the horizontal section of the power divider and repeat the S parameter simulation. If the result is not satisfactory, we increase the number of quarter wavelength sections (N) and repeat the procedure until we reach a design that satisfies all the requirements.

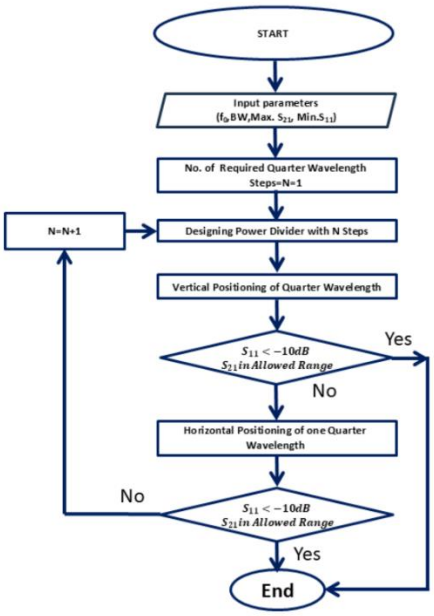

Fig. 4. Flowchart of the design procedure of the power dividers of each section.

Figure 5(a) shows the overall view and port numbers (P_1 to P_9) of a three-layer divider network that we design on the basis of the flowchart of Fig. 4 for feeding an eight branch SSPP antenna for the frequency range of 11.7- 12.2 GHz. Figures 5(b,c,d) show the number of steps and locations of the quarter-wavelength impedance convertors of the dividers and their dimensions for each of the three sets of microstrip 1:2 power dividers (Div1, Div2, and Div3). Table II shows the values of various sections of this divider network. The right angles of the microstrip bends of the power dividers are chamfered as shown in Figs. 5(b,c,d). All the input and output impedances of the ports shown in Fig. 5 are 50 ohms.

3. The Simulated and Experimental Evaluation

3.1. Simulated and Fabricated Results

Figure 6 shows the optimized magnitude of the simulated S_{11} and S_{12} of the microstrip to CPW transition circuit shown in Fig. 3. Figure 7 shows the magnitude of the simulated reflection and transmission coefficients of the divider network of Fig. 5(a).

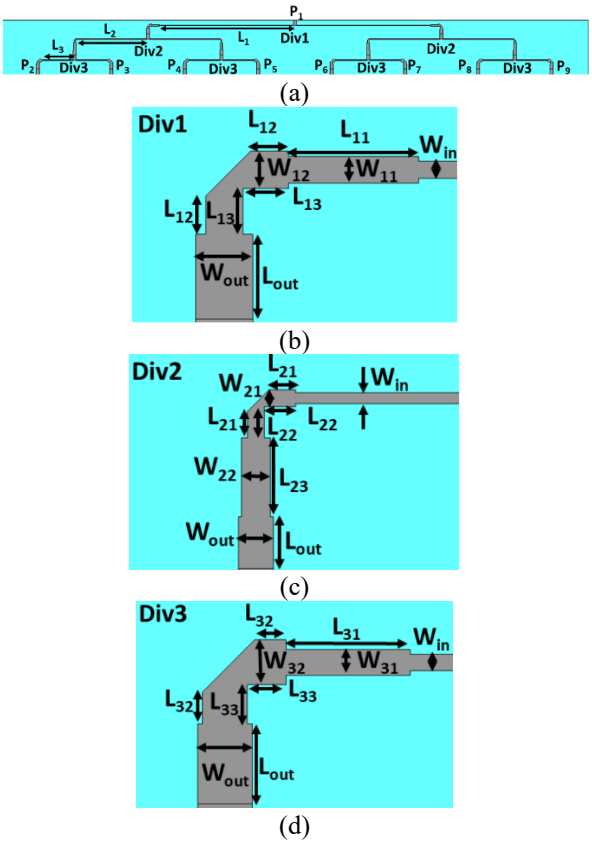

Fig. 5. (a) The overall view of a three-layer divider network, (b) Div1, (c) Div2, (d) Div3.

Table II. Values of Fig. 5 parameters, all in millimetres.

L_1	L_{11}	L_{12}	L_{13}	L_{out}	W_{in}
70.8	3.87	1.13	1.37	2.5	0.5
W_{11}	W_{12}	W_{out}	L_2	L_{21}	L_{22}
0.8	1.1	1.7	35.94	1.3	1.54
L_{23}	L_{wg}	W_{21}	W_{22}	L_3	L_{31}
3.8	0.2	0.8	1.4	12.74	3.87
L_{32}	L_{33}	L_{34}	L_{35}	W_{31}	W_{32}
0.97	1.2	1.2	0.97	0.8	1.4

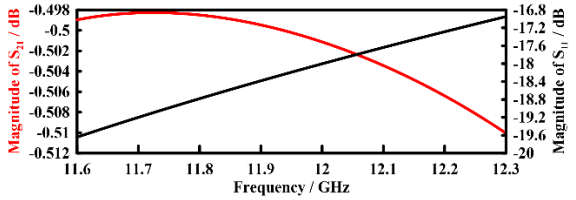

Fig. 6. The optimized magnitude of the simulated S_{11} and S_{21} of the microstrip to CPW transition circuit shown in Fig. 3.

Figure 7 shows good reflection (S_{11}<-12 dB) and insertion loss (S_{i1}, i=2 to 9) of less than 11.1 dB, which is only 2.07 dB higher than the theoretical value of S_{i1} (9.03 dB) for a 1:8 divider network. The simulated phase difference of the transmission coefficients between the output ports is less than the negligible value of 4.5°, which shows that all the output signals are almost in phase, as required. As shown in Fig. 7, the output power depends on the amount of coupling between the divider branches, and the ports located on the left and right sides of the divider (P_2, P_3, P_8 and P_9) have the highest transmission coefficients because they have the lowest coupling with the input Div1 branches. Owing to symmetry, three categories of mutual isolation can be seen between the output ports of the divider network of Fig. 5, as shown in Fig. 8. We avoid showing the isolation of other ports to keep the graph more readable.

As shown in Fig. 8, the lowest isolation category is between the adjacent ports of Div3 (S_{23}), which is between -8 dB and -2.5 dB. The middle category isolation is better than -10 dB, and the highest isolation is better than -19 dB. Table III lists the three categories of isolation between output ports. As in S parameters representing the isolation, S_{ij}=S_{ji}, only S_{ij} parameters are listed in each category in Table III.

One way to practically evaluate any power divider network's effectiveness, is to compare the maximum measured radiation gain of a multibranch SSPP antenna array fabricated with that divider network, against the simulated gain of a single-branch of the same antenna used in that array. This method will vindicate both the characteristics of the power divider network and its matching with the antenna array branches. We use our unpublished recent work that studies an eight-branch

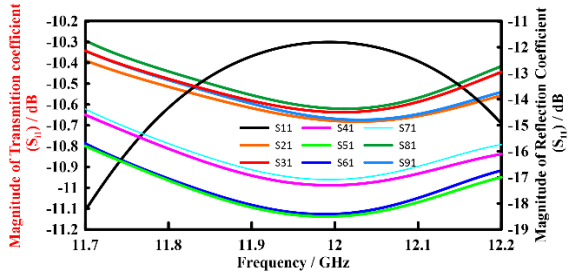

Fig. 7. The magnitude of the simulated reflection and transmission coefficients of the divider network of Fig. 5(a).

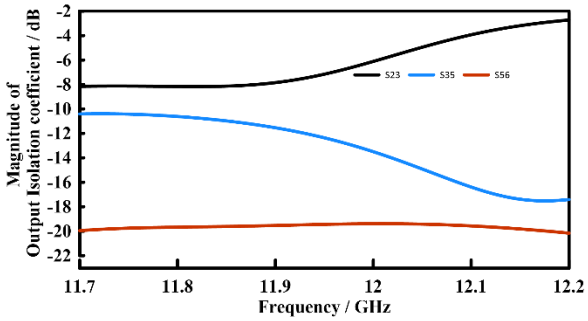

Fig. 8. The magnitude of three categories of the simulated isolation of the divider network ports of Fig. 5(a).

Table III. The three categories of mutual isolation between output ports

Category 1	S_{23}	S_{45}	S_{67}	S_{89}				
Category 2	S_{24}	S_{25}	S_{34}	S_{35}	S_{68}	S_{69}	S_{78}	S_{79}
Category 3	S_{26}	S_{27}	S_{28}	S_{29}	S_{36}	S_{37}	S_{38}	S_{39}
	S_{46}	S_{47}	S_{48}	S_{49}	S_{56}	S_{57}	S_{58}	S_{59}

SSPP antenna that uses our proposed divider network structure for this purpose. Figure 9(a) shows the top view, and Fig.9(b) shows the bottom view of one of the eight microstrip to CPW transition sections that we use to fabricate the power divider network for feeding the eight-branch array antenna. This structure allows juxtaposing multiple branches of antennas and their coplanar grounds without any unwanted collision between ground and neighbouring antennas and also provides required grounds for branches located in the non-lateral parts of structure. Figure 10(a) shows the complete top layer, and Fig. 10(b) shows the complete bottom layer of the fabricated power divider network of Fig. 5(a), together with all eight microstrip to CPW transition sections of Fig. 9 and eight SSPPs designed with a rectangular plasmonic metal-dielectric structure decorated by etching circular holes and explained in our unpublished recent work. The proposed novel combination allows direct electrical contact between adjacent CPW ground planes without crossing or affecting the rest of the elements. We use the Agilent 8720ET transmission/reflection network analyser to measure the S_{11} of the fabricated input network connected to the array antenna. Figure 11 shows the magnitude of the measured S_{11} parameter of the power divider network loaded with the eight branches of the SSPP antennas. As shown in Fig. 11, the measured bandwidth of the antenna is 0.98 GHz (11.536- 12.516 GHz), which is wider than the .5 GHz required bandwidth of the antenna (11.7- 12.2 GHz). Figure 12 shows the gain of a single branch and an eight-branch rectangular patch SSPP antenna with the ground at the top designed by the divider network of Fig. 10 and studied in our unpublished earlier work. In this paper we focus on divider network characteristics, and other eight-branch antenna parameters are presented in our unpublished recent work.

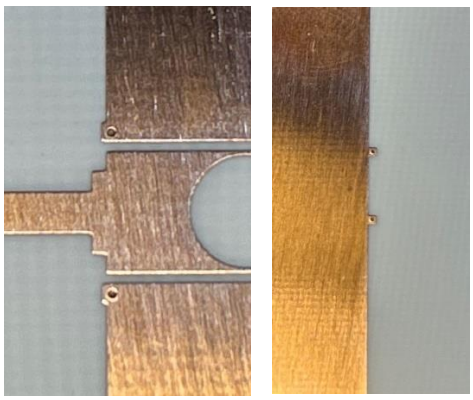

(a) (b)

Fig. 9. (a) Top view and (b) bottom view of one of the eight microstrip to CPW transition sections of the power divider network.

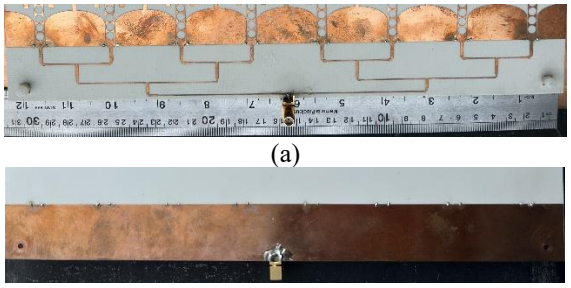

(a) (b)

Fig. 10. (a) Complete top layer and (b) complete bottom layer of the fabricated power divider network and microstrip to CPW transition used to feed eight branches of an SSPP antenna.

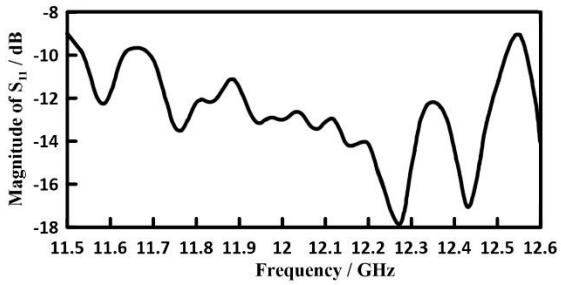

Fig. 11. Magnitude of the measured S_{11} of the fabricated input network loaded with eight antenna branches.

As shown in Fig. 12, the maximum gain increase of the eight-branch array antenna with ground at the top with respect to the simulated gain of a single-branch SSPP base antenna with the same parameters is 7.48 dB.

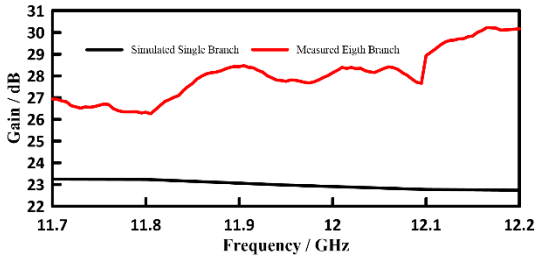

Fig. 12. Gain of a single branch and an eight-branch rectangular patch SSPP antenna with the ground at the top designed by the divider network of Fig. 10.

3.2. Discussion

Table IV shows the comparison of our proposed power divider network with two available similar works that include the power division network and SSPP antennas. It is clear that as the number of branches increases, the extended signal paths in microstrip waveguides and the additional dividers and lossy elements in large arrays inevitably introduce more losses, causing a more significant difference between the predicted and measured gain values. This deviation between the ideal and achieved results should be considered when we compare the performance of an eight-branch network with that of two- or four-branch networks. Although our proposed power divider network consists of seven 1:2 power dividers, eight microstrip to CPW transition sections, and a long microstrip traveling distance of more than 250 mm due to the large size of the antenna that imposes several inherent losses, the maximum gain increase of 7.48 dB, which is only 1.55 dB lower than the theoretical value of an ideal eight-branch array antenna (9.031 dB), shows promising results in comparison with the two- and four-branch power division networks shown in Table IV.

4. Conclusion

A novel and efficient complex microstrip power divider network with microstrip to CPW conversion for feeding arrays of arbitrary SSPP antennas with CPW input is proposed in this paper. Although individual components used in this paper can be found in previous papers, the main novelty of this paper is to find a special spatial arrangement that allows juxtaposing multiple branches of antennas and their coplanar grounds without any unwanted collision between grounds and neighbouring antennas and also providing the required grounds for branches located in the non-lateral parts of structure. A flowchart detailing the overall design methodology is also presented. The effectiveness of the proposed divider network is demonstrated by an increase of 7.48 dB in the measured array antenna gain of a fabricated eight-branch SSPP antenna with respect to the simulated single-branch radiation gain of the same antenna. Considering the inherent losses of several circuit elements and long microstrip distances that are necessary for feeding eight branches of the SSPP antenna, the value of the gain increase, which is only 1.55 dB lower than the theoretical value, vindicates the effectiveness of the structure. The fabricated structure also exhibits almost in-phase outputs with less than the negligible value of 4.5° phase difference between all ports and excellent impedance matching properties. Since a detached PEC or AMC ground plane

Table IV. Comparison of our proposed power divider network with two similar works

Reference	Number of Branches	M.M.A.F * (dB)	Diff. With Theory (dB)	Measured (S_{11}) better than (dB)
[20]	2	3	0	-9.5
[21]	4	5	1	-9.5
This Work	8	7.48	1.55	-10

* M.M.A.F: Maximum Measured Array Factor

can improve SSPP antenna performance more effectively than an attached ground, the proposed groundless design in the antenna section - which replaces the microstrip ground with a microstrip-to-CPW transition - offers superior suitability for SSPP antennas.

References

[1] H. Raether, “Surface Plasmons on Smooth and Rough Surfaces and on Gratings,” *Springer Tracts Mod. Phys.*, vol. 111, pp. 4–39, 1988, doi: 10.1007/BFb0048317.

[2] J. B. Pendry, L. Martín-Moreno, and F. J. Garcia-Vidal, “Mimicking surface plasmons with structured surfaces,” 2004. doi: 10.1126/science.1098999.

[3] R. S. Anwar, H. Ning, and L. Mao, “Recent advancements in surface plasmon polaritons-plasmonics in subwavelength structures in microwave and terahertz regimes,” *Digit. Commun. Networks*, vol. 4, no. 4, pp. 244–257, 2018, doi: 10.1016/j.dcan.2017.08.004.

[4] H. F. Ma, X. Shen, Q. Cheng, W. X. Jiang, and T. J. Cui, “Broadband and high-efficiency conversion from guided waves to spoof surface plasmon polaritons,” *Laser Photonics Rev.*, vol. 8, no. 1, pp. 146–151, 2014, doi: 10.1002/lpor.201300118.

[5] R. Garg, *Microstrip Antenna Design Handbook*. Artech House, 2001.

[6] Q. Le Zhang, Q. Zhang, and Y. Chen, “High-efficiency circularly polarised leakywave antenna fed by spoof surface plasmon polaritons,” *IET Microwaves, Antennas Propag.*, vol. 12, no. 10, pp. 1639–1644, 2018, doi: 10.1049/iet-map.2017.1054.

[7] Q. Le Zhang, Q. Zhang, and Y. Chen, “Spoof Surface Plasmon Polariton Leaky-Wave Antennas Using Periodically Loaded Patches above PEC and AMC Ground Planes,” *IEEE Antennas Wirel. Propag. Lett.*, vol. 16, pp. 3014–3017, 2017, doi: 10.1109/LAWP.2017.2758368.

[8] D. Liao, Y. Zhang, and H. Wang, “Wide-Angle Frequency-Controlled Beam-Scanning Antenna Fed by Standing Wave Based on the Cutoff Characteristics of Spoof Surface Plasmon Polaritons,” *IEEE Antennas Wirel. Propag. Lett.*, vol. 17, no. 7, pp. 1238–1241, 2018, doi: 10.1109/LAWP.2018.2841006.

[9] J. Wang, L. Zhao, Z. C. Hao, and T. J. Cui, “An ultra-thin coplanar waveguide filter based on the spoof surface plasmon polaritons,” *Appl. Phys. Lett.*, vol. 113, no. 7, 2018, doi: 10.1063/1.5045069.

[10] V. Rabinovich and N. Alexandrov, *Antenna arrays and automotive applications*., pp 27, Fig. 2.3 New York, 2013. doi: 10.1007/978-1-4614-1074-4.

[11] H. T. Xu *et al.*, “An ultra-wideband out-of-phase power divider based on odd-mode spoof surface plasmon polariton,” *Int. J. RF Microw. Comput. Eng.*, vol. 31, no. 4, pp. 1–8, 2021, doi: 10.1002/mmce.22583.

[12] J. Wang, L. Zhao, Z.-C. Hao, X. Shen, and T. J. Cui, “Splitting spoof surface plasmon polaritons to different directions with high efficiency in ultra-wideband frequencies,” *Opt. Lett.*, vol. 44, no. 13, pp. 3374–3377, 2019, doi: 10.1364/ol.44.003374.

[13] S. Zhou *et al.*, “Spoof Surface Plasmon Polaritons Power Divider with large Isolation,” *Sci. Rep.*, vol. 8, no. 1, pp. 1–8, 2018, doi: 10.1038/s41598-018-24404-0.

[14] A. K. Horestani and Z. Shaterian, “Ultra-wideband balun and power divider using coplanar waveguide to microstrip transitions,” *AEU - Int. J. Electron. Commun.*, vol. 95, pp. 297–303, 2018, doi: 10.1016/j.aeue.2018.08.024.

[15] A. N. Ghazali, M. Sazid, and S. Pal, “Multiple passband transmission zeros embedded compact UWB filter based on microstrip/CPW transition,” *AEU - Int. J. Electron. Commun.*, vol. 129, no. November 2020, p. 153549, 2021, doi: 10.1016/j.aeue.2020.153549.

[16] A. N. Ghazali, M. Sazid, and S. Pal, “Dual band notched UWB-BPF based on hybrid microstrip-to-CPW transition,” *AEU - Int. J. Electron. Commun.*, vol. 86, pp. 55–62, 2018, doi: 10.1016/j.aeue.2018.01.009.

[17] P. Goel and K. J. Vinoy, “A low-cost phased array antenna integrated with phase shifters cofabricated on the laminate,” *Prog. Electromagn. Res. B*, no. 30, pp. 255–277, 2011, doi: 10.2528/PIERB11041105.

[18] M. Siasifar, A. Keshtkar, and S. Amiri, “Optimum Patch Selection for Wideband Planar Spoof Surface Plasmon Polaritons Ku-Band Satellite Receive Antenna,” in *2024 11th International Symposium on Telecommunications (IST)*, 2024, pp. 135–140. doi: 10.1109/IST64061.2024.10843596.

[19] A. Tiwari, U. Pattapu, and S. Das, “A wideband 1:2 T-junction power divider for antenna array with optimum results,” *2018 3rd Int. Conf. Microw. Photonics, ICMAP 2018*, vol. 2018-Janua, no. Icmap, pp. 1–2, 2018, doi: 10.1109/ICMAP.2018.8354594.

[20] D. Wei, J. Li, J. Yang, Y. Qi, and G. Yang, “Wide-Scanning-Angle Leaky-Wave Array Antenna Based on Microstrip SSPPs-TL,” *IEEE Antennas Wirel. Propag. Lett.*, vol. 17, no. 8, 2018, doi: 10.1109/LAWP.2018.2855178.

[21] J. Wang, K. Xu, X. Kong, R. Xu, and L. Zhao, “Wide-Angle Beam-Scanning Leaky-Wave Antenna Array Based on Hole Array SSPPs,” *IEEE Antennas Wirel. Propag. Lett.*, vol. 22, no. 7, pp. 1731–1735, 2023, doi: 10.1109/LAWP.2023.3262567.